

# A Computational Study into the Effect of Design Parameters on Ignition Timing and Emission Characteristics of HCCI Engine in Internal Combustion Engines Fuelled with Isooctane

Fridhi Hadia, Soua Wadhah, Hidouri Ammar, Omri Ahmed

**Abstract**—In order to understand the auto-ignition process in a HCCI engine better, the influence of some important parameters on the auto-ignition is investigated. The inlet temperature, the inlet pressure, and the compression ratio were varied and their influence on the ignition delays and emission characteristics were studied. The inlet temperature was changed from 400 K to 460 K (in step of 15 K), the inlet pressure from 0.9 to 3 atm, while the compression ratio varied from 15 to 23. The fuel that was investigated is isooctane. The inlet temperature, the inlet pressure, and the compression ratio appeared to decrease the ignition delays, with the inlet pressure having the least influence and the compression ratio the most. The effect of these parameters on emissions' characteristics were also investigated. Results indicate that increasing the compression ratio results in increasing the concentration of all the species.

**Keywords**—Compression Ratio, intake temperature, intake pressure, HCCI engine, isooctane.

## I. INTRODUCTION

HCCI engines combine the best features of conventional SI and CI engines: the pre-mixed air–fuel mixture is inducted as in conventional SI engine and the auto-ignition process takes place as in the conventional CI engine. Thus, HCCI is the best alternative combustion technology to produce near zero NO<sub>x</sub> and soot emissions with high fuel efficiency [1]–[4].

A review has been prepared to study the effect of compression ratio, intake temperature and intake pressure on the ignition timing and emission characteristics of IC engine.

The Compression Ratio (CR) is an equally important design parameter that has a momentous effect on performance and emission characteristics [5]. The effects of varying CR on engine performance have been widely studied. This is due to the fact that operating at different CRs; the engine performance can be optimized for a full range of driving conditions. Y. Hüseyin et al. [5] studied the effect of ethanol–gasoline blends on engine performance and exhaust emissions

by varying the CR. They concluded that both the performance and emission characteristics were found to be good at higher CR. In the same way, C. Rodrigo [6] investigated the effect of CR on an ethanol/gasoline blend and hydrous ethanol fuelled engine performance.

This paragraph treats the effect of intake charge temperature on HCCI combustion. It has been extensively reported by many researchers. In 1983, Najt et al. found that HCCI of lean mixtures could be achieved in a SI engine that has a low CR with elevated intake charge temperatures (572–772°C) [7]. In general, the intake charge temperature has a strong influence on the HCCI combustion timing. Iida et al. also indicated that an increase in intake charge temperature (from 297 K to 355 K) increased the peak temperature after compression and advanced the HCCI combustion on-set [8].

In the following, we are going to underline the research works that have been investigated in the field of injection pressure in I.C engine. A review of fuel injection system of I.C engine has been described in the following orders. Cenk Sayin et al. [9] investigated the effect of injection pressure (IP) on the performance and emissions of a DI diesel engine using bio-diesel (5%, 20%, 50%, and 100%) blended-diesel fuel. They found that HC, and CO emissions decreased and NO<sub>x</sub> emissions increased with the increase in IP for all the fuel blends. S.S. Karhale et al. [10] investigated the performance of Karanja methyl ester and its blends with diesel from 20%, 40% and 60% by volume for running a diesel engine. The engine was tested in two injection pressures 180 kg/cm<sup>2</sup> and 245 kg/cm<sup>2</sup> and temperatures of 30, 50 and 70°C. They concluded that injection pressure and fuel temperature have significant effects on engine performance parameters. Sukumar et al. [11] studied the effect of injection pressures (200, 220 and 240 bar) on performance, emissions and combustion characteristics of the DI Diesel engine. In their study, a high linolenic linseed oil methyl ester has been investigated. They found that, at 240 bar injection pressure, the thermal efficiency was improved with increased emissions. This may probably be due to the changes in the fuel spray structure which affects combustion. Thermal efficiency at 200 bar injection pressure was comparatively lower than that of diesel.

Fridhi H. is with the Research Unity of Materials, Energy and Renewable energies MEER, Gafsa Faculty of Science, Zaroug Gafsa 2112, Tunisia (Corresponding author; e-mail: fridhi.hadia@yahoo.com).

Soua Wadhah, Hidouri Ammar and Omri Ahmed are with the Research Unity of Materials, Energy and Renewable energies MEER, Gafsa Faculty of Science, Zaroug Gafsa 2112, Tunisia (e-mail: souw@yahoo.fr, ammar-hidouri@yahoo.fr, ahm206@yahoo.fr)

## II. NUMERICAL INVESTIGATION

## A. Overview of Simulation Software

CHEMKIN [12] is a powerful set of software tools for solving complex chemical kinetics problems. It is used to study the reacting flows, such as those found in combustion, catalysis, chemical vapor deposition, and plasma etching. CHEMKIN consists of rigorous gas-phase and gas-surface, chemical kinetics in a variety of reactor models that can be used to represent the specific set of systems of interest (Fig. 1). CHEMKIN has several models representing simple geometries. These models are used to test the different reaction mechanisms of combustion. In our work, we have used the ICE (Internal Combustion Engine) model.

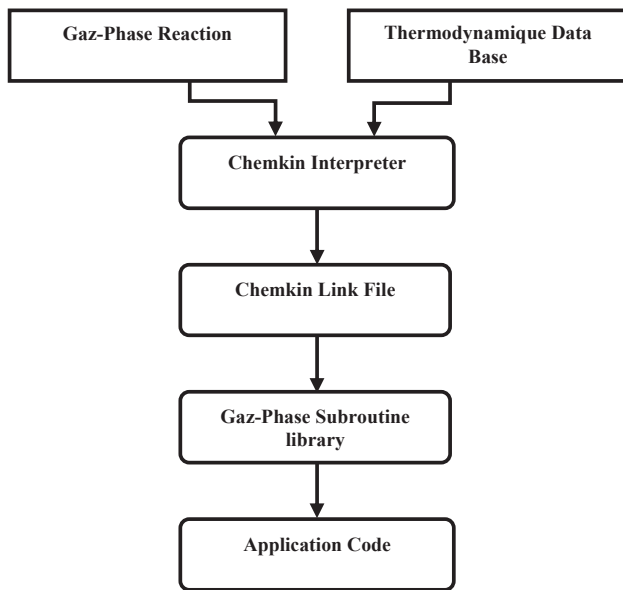


Fig. 1 Chemkin package working flow diagram

## B. Engine Geometric Parameters

Fig. 2 shows the geometry of the piston and crank mechanisms.

The crank radius,  $a$ , is defined as half the stroke length,  $L$

$$a = \frac{L}{2} \quad (1)$$

and the ratio of connecting rod length to crank radius is given by

$$R = \frac{l}{a} \quad (2)$$

The rotational speed of the engine is

$$w = \frac{2\pi N}{60} \quad (3)$$

where  $N$  is the engine speed in rotations per minute (RPM). For a flat piston crown, the area is given by

$$A_p = \frac{\pi B^2}{4} \quad (4)$$

where  $B$  represents the bore diameter of the engine. When the piston is at TDC, the clearance volume is

$$V_c = \frac{V_d}{(R_c - 1)} \quad (5)$$

where  $V_d$  is the displacement volume and  $R_c$  is the CR, which are given as

$$V_d = A_p L \quad (6)$$

$$R_c = \frac{\text{maximum cylinder volume}}{\text{minimum cylinder volume}} = \frac{V_d + V_c}{V_c} \quad (7)$$

Then, the instantaneous cylinder volume at any crank angle location can be determined from

$$V = V_c + A_p(l + a - s) \quad (8)$$

where  $s$  is the distance between crank axis and piston pin axis, which is given by

$$s = a \cos \theta + \sqrt{(l^2 - a^2 \sin^2 \theta)} \quad (9)$$

After manipulation of (8) and (9), the instantaneous cylinder volume is

$$V = V_c \left[ 1 + \frac{R_c - 1}{2} \left( R + 1 - \cos \theta - \sqrt{R^2 - \sin^2 \theta} \right) \right] \quad (10)$$

with the rate of change of volume

$$\frac{dV}{d\theta} = V_c \left[ \frac{R_c - 1}{2} \sin \theta \left( \frac{1 + \cos \theta}{\sqrt{R^2 - \sin^2 \theta}} \right) \right] \quad (11)$$

While the time derivative of the volume is:

$$\frac{d(V)}{dt} = \Omega \left( \frac{R_c - 1}{2} \right) \sin \theta \left[ \frac{1 + \cos \theta}{\sqrt{R^2 - \sin^2 \theta}} \right] \quad (12)$$

where  $\Omega$  the rotation rate of the crank arm is given by:

$$\Omega = \frac{d\theta}{dt} \quad (13)$$

## C. Heat Transfer Calculation between Gases and In-Cylinder Walls

Fig. 3 illustrates both the convective and radioactive components, the heat transfer between gas and in-cylinder

wall, conduction through the combustion chamber wall, and convection to the coolant.

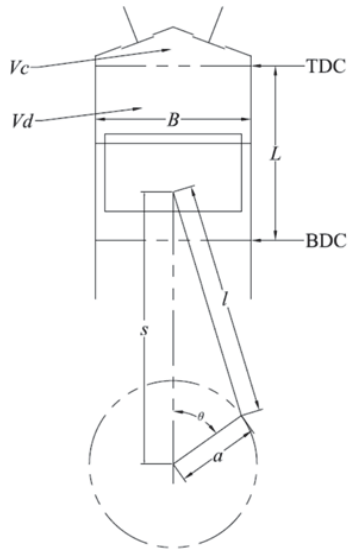


Fig. 2 Engine geometry of the piston and crank mechanisms:  $l$ : The connecting rod length;  $a$ : the crank arm radius;  $B$ : the bore;  $s$ : the distance between crank axis and wrist pin axis;  $L$ : stroke length;  $V_c$ : The clearance volume;  $V_d$ : the displacement volume

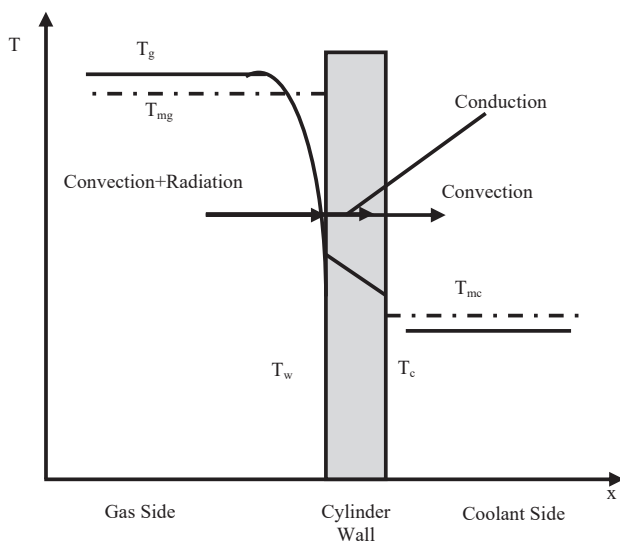


Fig. 3 Schematic of the overall heat transfer process in the cylinder [12]  $T_g$ : instantaneous in-cylinder gas temperature (K);  $T_w$ : surface temperature of combustion chamber wall (K);  $T_c$ : surface temperature of wall of coolant side (K);  $T_{mg}$ : Mean gas temperatures;  $T_{mc}$ : Mean coolant temperatures

The convective heat transfer coefficient between the gas and cylinder wall can be obtained from the generalized heat transfer correlation in terms of a Nusselt number.

$$Nu_h = a Re^b Pr^c \quad (14)$$

where  $Nu_h$  the Nusselt number,  $Re$  the Reynolds number and  $Pr$  the Prandtl number. These are defined according to:

$$Nu_h = \frac{hD}{\lambda} ; Re = \frac{\rho w D}{\mu} \quad \text{and} \quad Pr = \frac{c_p \mu}{\lambda}$$

$D$  is the cylinder diameter;  $h$  is defined as a heat transfer coefficient;  $c_p$  is the specific heat at constant pressure;  $\lambda$  is the thermal conductivity;  $\mu$  is dynamic viscosity;  $\rho$  is density;  $w$  is the average cylinder gas speed;  $v$  is kinematic viscosity (m<sup>2</sup>/s) and  $r$  is radial distance from the cylinder axis (m).

The heat transfer correlation coefficients (denoted by  $a$ ,  $b$  and  $c$ ) were taken from reference [12] at Table I.

In particular, the Woschni [13] correlation has frequently been used in the heat transfer studies with proper constants in today's SI and diesel engines, and also it has been correlated conveniently even for HCCI engines recently [14].

Instantaneous heat transfer coefficient adopted from Woschni [13] is calculated by:

$$h(\theta) = 3.26 P(\theta)^b T_g(\theta)^{0.75-1.62} D^{b-1} w(\theta)^b \quad (15)$$

He assumed that the "b exponent" is 0.8 where  $w$  is the average cylinder gas speed given by Woschni Correlation [13] with a more accurate estimation.

$$w = \left[ C_{11} \bar{S}_p + C_2 \frac{V_d T_i}{P_i V_i} (P - P_{motored}) \right] \quad (16)$$

$p$  is the instantaneous cylinder pressure,  $p_i$ ,  $V_i$ ,  $T_i$  are the working fluid pressure, volume, and temperature at some reference state (say inlet valve closing or start of combustion),  $v_{swirl}$  is the swirl velocity,  $V_d$  is the displacement volume,  $p_{motored}$  is the motored cylinder pressure at the same crank angle as  $p$ .

- For the gas exchange process  $C_{11}=6.18$ ,  $C_2=0$ .
- For the compression process  $C_{11}=2.28$ ,  $C_2=0$ .
- For combustion and expansion processes  $C_1=2.28$ ,  $C_2=3.24 \cdot 10^{-3}$ .
- For engines with swirl, cylinder averaged gas velocities were fitted with:

$$w = \left[ \left( C_{11} + C_{12} \frac{v_{swirl}}{\bar{S}_p} \right) \bar{S}_p + C_2 \frac{V_d T_i}{P_i V_i} (P - P_{motored}) \right] \quad (17)$$

- For the gas exchange period:  $C_{11}=6.18$  and  $C_{12}=0.417$
- For the rest of the cycle:  $C_{11}=2.28$  and  $C_{12}=0.308$

The Woschni [13] correlation coefficients used in this study, (denoted by  $C_{11}$ ,  $C_{12}$  and  $C_2$ ), were taken from reference [13] at Table II.

The engine is assumed to have a bore of 72 mm, stroke of 120.65 mm and Ratio of the Connecting Rod length to crank Radius of 3.59. Five CRs are analyzed: 15; 17; 19; 21 and 23, and the Displaced Volume is 587.622 cm<sup>3</sup>. The fuel is

gasoline (C<sub>8</sub>H<sub>18</sub>). The averaged cylinder wall temperature is fixed at 415 K. The engine specification used for this work is shown in Table III.

TABLE I  
HEAT TRANSFER CORRELATION COEFFICIENTS [13]

Coefficient	Values
a	0.035
b	0.071
c	0.0

TABLE II  
THE WOSCHNI CORRELATION COEFFICIENTS [13]

Coefficient	Values
C11	2.28
C12	0.308
C2	0.324

### III. RESULTS AND DISCUSSION

#### A. Model Validation

The engine model was validated by comparison between our study and Yambin result's [14] for five intake temperature cases (480, 485, 492.5, 497.5, and 510 Kelvin). Our results are validated and well suited up with those of Yambin studies. This study is extended to evaluate the effect of CR, Intake Temperature (IT) and Intake Pressure (IP) on ignition timing and emissions' characteristics of HCCI.

TABLE III  
GEOMETRY OF ENGINE AND FIXED ENGINE OPERATING PARAMETERS

Parameters	Setting
Displaced Volume	587.622 cm <sup>3</sup>
Bore ×stroke	72mm×120.6 mm
Ratio of the Connecting Rod length to crank Radius	3.59
Intake temperature (K)	400-460
Wall temperature (K)	415
Intake pressure (atm)	0.9-3
Engine Speed (rpm)	1000.0
CR	15 – 23
Fuel	Isocetane

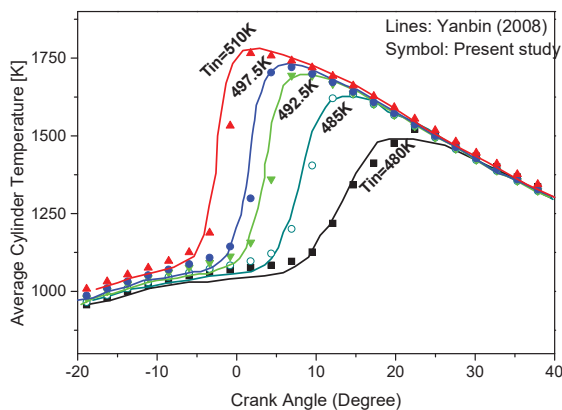


Fig. 4 Comparison between the present study and [15]

Table IV illustrates the values of the parametric variables of CR; Inlet Temperatures (IT) and Inlet Pressures (IP). The

reference conditions for the engine is 18 for CR, 430 K for IT and 1.065 atm for IP.

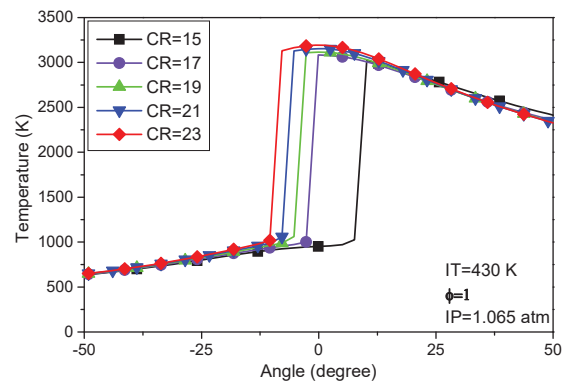
TABLE IV  
PARAMETER VARIABLES

Parameter variable	CR	IT (K)	IP (atm)
1	15	400	0.9
2	17	415	1.2
3	19	430	1.5
4	21	445	2
5	23	460	3

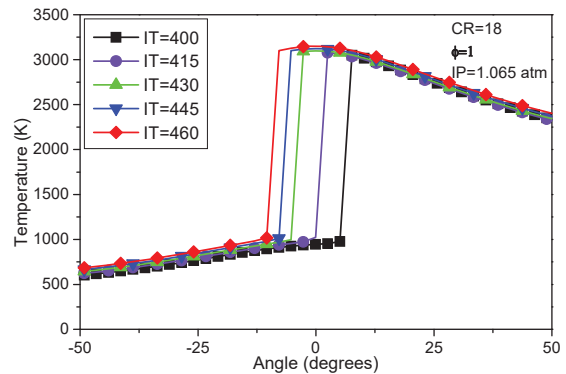
#### B. Effects of Design Parameters on Ignition Timing

##### 1. Temperature

Figs. 5 (a)–(c) show the effects of CR, IT and IP on temperature variations with crank angle in a stoichiometric mixture. When CR, IT, and IP are considered together, the effects of IT on cylinder temperature is limited compared to the other parameters. These figures illustrate that as the CR, IT and IP increase, the ignition timing advances.



(a)



(b)

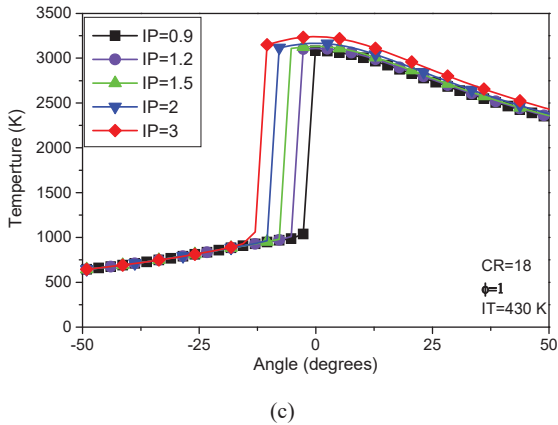
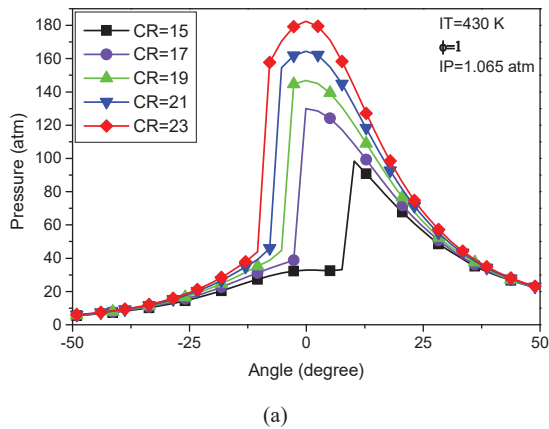


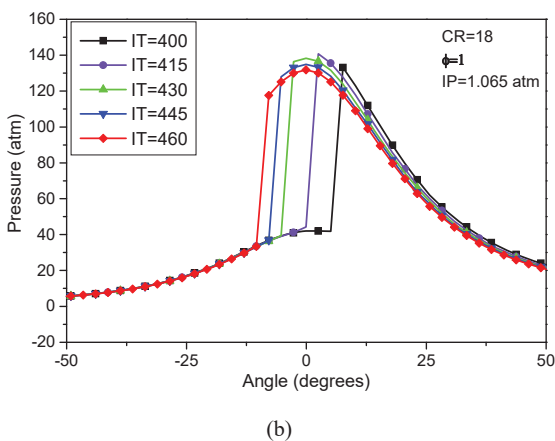
Fig. 5 Variation of Temperature versus crank angle for different CR (a); Inlet Temperatures (IT) (b); and Inlet Pressures (IP) (c)

2. Pressure

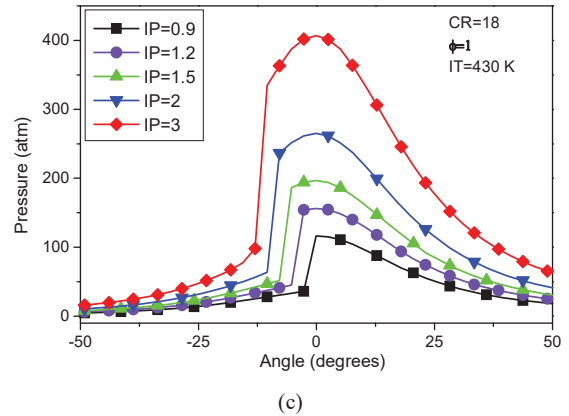
Figs. 6 (a)–(c) illustrate the effects of CR, IT and IP on pressure variations versus crank angle. The pressure increases with the rise in CR, IP, but decreases with IT. The reason of this decrease in the peak pressure is due to that less air enters into the cylinder.



(a)



(b)

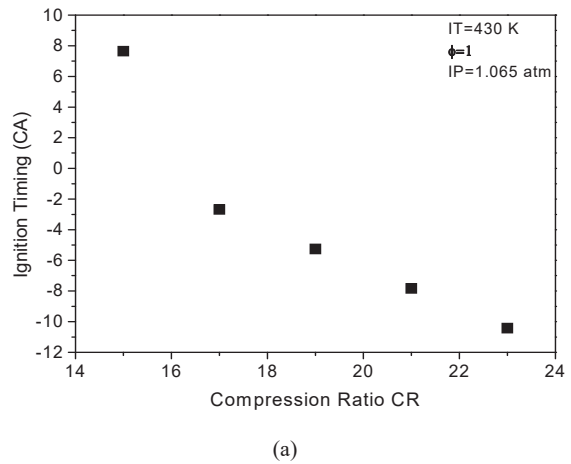


(c)

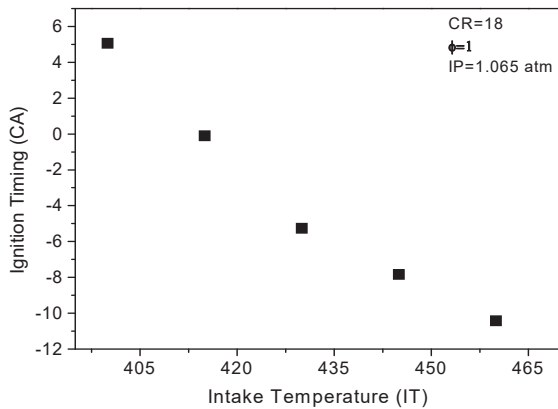
Fig. 6 Variation of Pressure versus crank angle for different CR (a); Inlet Temperatures (IT) (b); and Inlet Pressures (IP) (c)

3. Ignition Timing

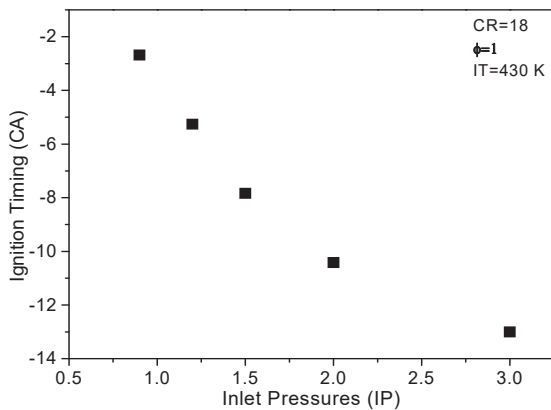
The effects of the inlet temperature, inlet pressures and the CR on the ignition timing were shown in Fig. 7. The data were obtained from the temperature traces showed in Figs. 5–6. It can be seen that these three parameters appeared to decrease the ignition timing with the inlet pressure having the least influence and the CR the most one. The combustion process does not occur for the CR equal and lower than 15. By increasing in the inlet pressure during the combustion of Isooctane, the ignition delay time decreases. This is because at high pressure the fuel-air mixture density is increased which results in proper mixing in turn shortens ignition delay times. A critical minimum value of Intake Temperature exists, which is 392 K, below it, ignition timing becomes infinite and the combustion process does not occur.



(a)



(b)



(c)

Fig. 7 Effect of CR (a); Inlet Temperatures (IT) (b); and Inlet Pressures (IP) (c) on the ignition timing of HCCI engine

### C. Effects of Design Parameters on Emission Characteristics

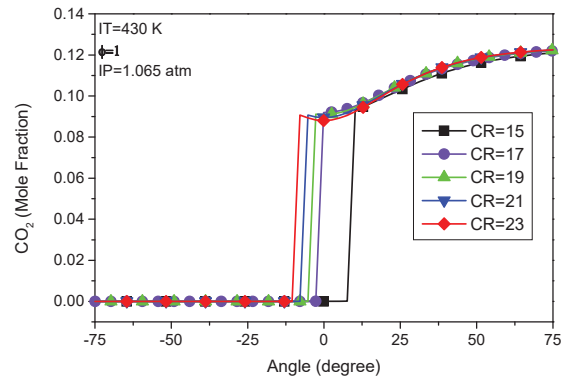
Emission of different exhaust gas species ( $\text{NO}_x$ ,  $\text{CO}_2$ , and  $\text{CO}$ ) with varying CR, IT and IP are presented in this section. In order to investigate their effect on emission characteristics, different values of these parameters are given in Table IV.

#### 1. Carbon Dioxide ( $\text{CO}_2$ ) Emissions

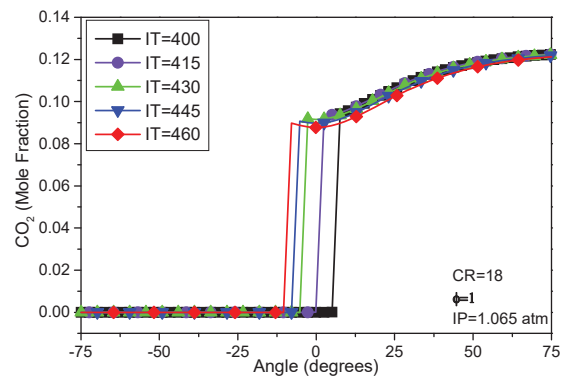
$\text{CO}_2$  is a normal product of combustion. Ideally, combustion of a hydrocarbon fuel should produce only  $\text{CO}_2$  and water ( $\text{H}_2\text{O}$ ). Fig. 8 describes the effect of CR, Inlet Temperatures (IT) and Inlet Pressures (IP) on  $\text{CO}_2$  emissions.

The effect of CR on  $\text{CO}_2$  emission is shown in Fig. 8 (a). The  $\text{CO}_2$  emission increases by increasing the CR. The increasing of CR leads to a high temperature and pressure which increases  $\text{CO}_2$ . This numerical study demonstrates that with a CR equal to 23, a maximum  $\text{CO}_2$  emission has been reached. However, a lowest emission of  $\text{CO}_2$  has been reached with CR equal to 15. The concentration of CO with various intake temperatures is shown in Fig. 8 (b).  $\text{CO}_2$  emissions appeared to have the opposite trend, with the lowest  $\text{CO}_2$  emissions corresponding to the highest temperature.  $\text{CO}_2$

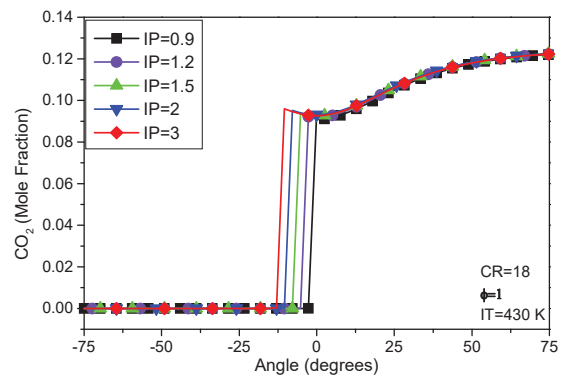
emissions increase also with IP indicating better combustion at higher IPs (Fig. 8 (c)).



(a)



(b)



(c)

Fig. 8  $\text{CO}_2$  mole fraction versus Crank angle for different CR (a); Inlet Temperatures (IT) (b); and Inlet Pressures (IP) (c)

#### 2. Carbon Monoxide (CO) Emissions

CO emission is toxic and must be controlled. CO emission is produced either directly or indirectly by combustion of fuels. In the ideal combustion process, carbon (C) and oxygen ( $\text{O}_2$ ) combine to produce  $\text{CO}_2$ . Incomplete combustion of carbon leads to CO formation. The formation of CO takes



place when the oxygen presented during combustion is insufficient to form  $\text{CO}_2$ . CO emissions results are presented in Figs. 7 (a)-(c). The effect of CR; Inlet Temperatures (IT) and Inlet Pressures (IP) on Carbon-Mono-Oxide (CO) is described in this figure. According to Fig. 7 (b), an important result from this study is that at lower inlet temperatures, a significant CO reduction was observed. With increase in IP, Fig. 7 (c), the fuel atomization happens efficiently. This results proper burning of the fuel and the production of carbon particles is reduced.

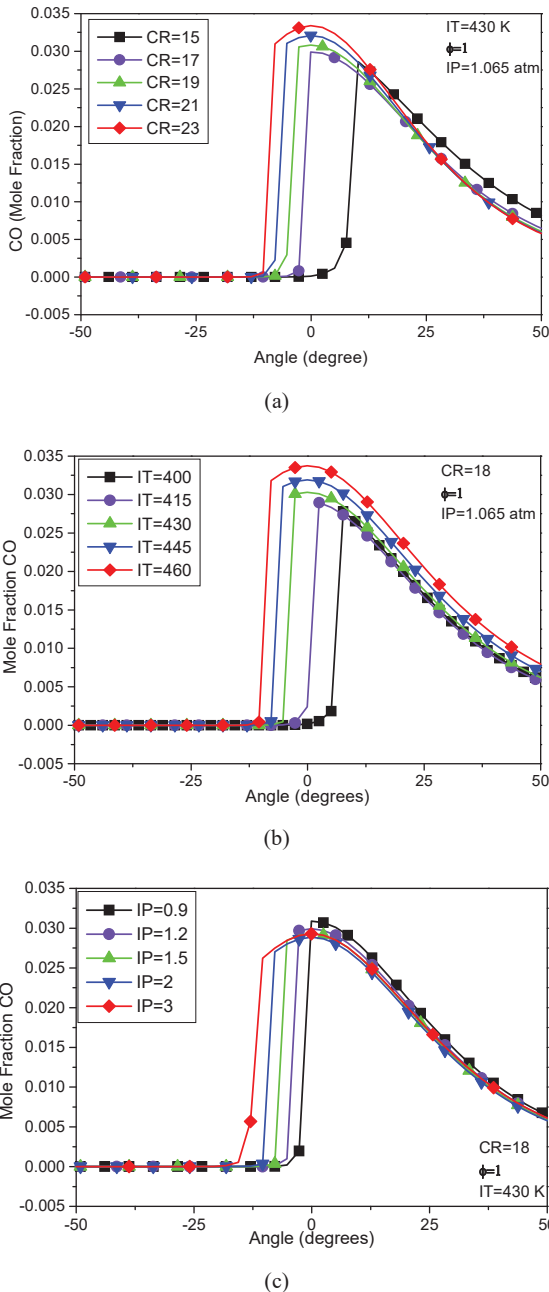


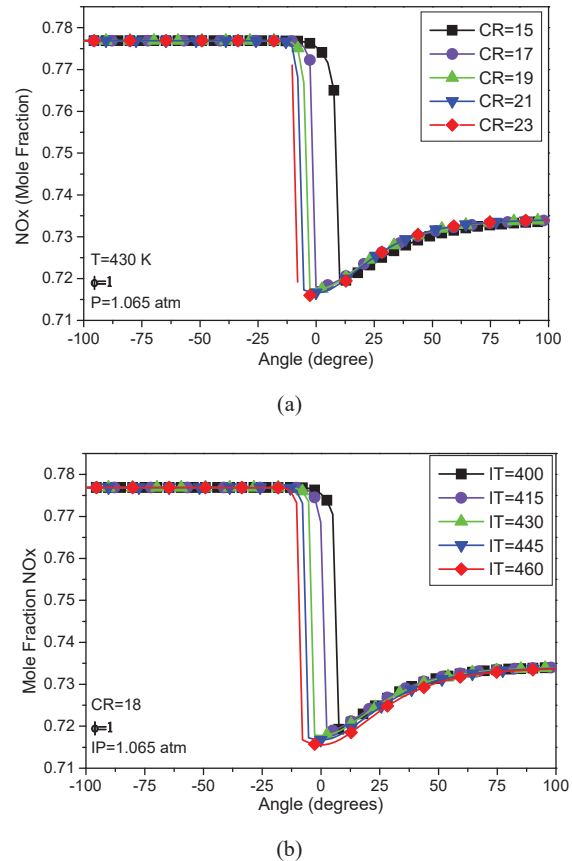
Fig. 9 CO mole fraction versus Crank angle for different CR (a); Inlet Temperatures (IT) (b); and Inlet Pressures (IP) (c)

### 3. Nitrogen Oxides (NO<sub>x</sub>) Emissions

The oxides of nitrogen in the exhaust emissions contain nitric oxide (NO) and nitrogen dioxide (NO<sub>2</sub>). The formation of NO<sub>x</sub> is highly dependent on three main factors [15]-[17]:

- peak temperature in-cylinder,
- duration of time that the cylinder gases exposed to higher temperatures
- the oxygen content during combustion

Fig. 10 (a) indicates the variations of NO<sub>x</sub> emissions for different CR. The most significant factor that causes NO<sub>x</sub> formation is high combustion temperatures. And the combustion temperature increases with the increasing of the CR. So as the CR increases, the formation of nitrogen oxides will increase. According to Fig. 10 (b), for the difference of intake temperature, a small reduction in NO<sub>x</sub> emissions also observed at lower initial temperatures. Fig. 10 (c) shows the effect of fuel injection pressure on NO<sub>x</sub> pollution versus Crank angle. It can be seen that with increasing injection pressure, NO<sub>x</sub> increases too. By increasing injection pressure, fuel particles became smaller and in fact atomization of fuel will get better and area of pre-mixing is being faster.



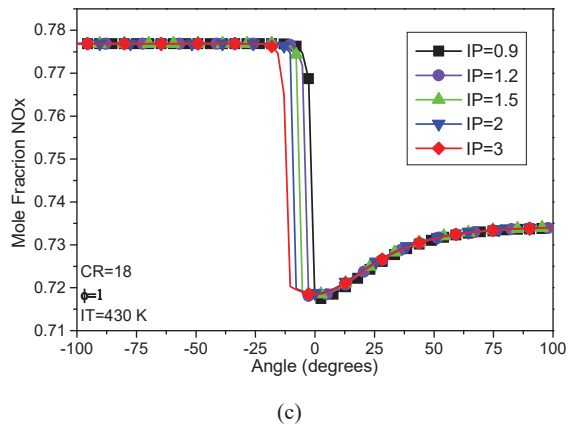


Fig. 10 NOx mole fraction versus Crank angle for different CR (a); Inlet Temperatures (IT) (b); and Inlet Pressures (IP) (c)

#### IV. CONCLUSION

The characteristics of a HCCI engine for a range of intake temperatures, intake pressure and CRs were investigated in a HCCI engine using iso-octane as a fuel. After studying the data, the following conclusions were reached:

- NO<sub>x</sub>, CO, and CO<sub>2</sub> emissions are all strongly dependent on CR, intake temperature (IT) and intake pressure
- CO<sub>2</sub> emissions were only affected by temperature and pressure variations, minimizing at high temperature, low pressure conditions.
- NO<sub>x</sub> emissions also responded mostly to varying pressures and temperatures. NO<sub>x</sub> is greatly reduced by lowering the intake temperature.
- With the increase in CR, the temperature reached is also high, so less CO emissions but, this effect increased NO<sub>x</sub> emission.
- The increased IT causes more time for carbon oxidation and leads to higher temperatures during the expansion stroke and so CO reduces.

The increased IP provides more surface area and better mixing with air and this effect improves combustion. CO emissions decreased and NO<sub>x</sub> emissions increased with the increase in IP.

#### REFERENCES

- [1] W. Ying, H. Li, Z. Jie, and Z. Longbao. "Study of HCCI-DI combustion and emissions in a DME engine," *Fuel*, vol. 88, no 11, pp. 2255-2261, 2009.
- [2] M. Fathi, R. K. Saray and M. D. Checkel. "The influence of Exhaust Gas Recirculation (EGR) on combustion and emissions of n-heptane/natural gas fueled Homogeneous Charge Compression Ignition (HCCI) engines," *Applied Energy*, vol. 88, no 12, pp. 4719-4724, 2011.
- [3] J. Jang, Y. Lee, C. Cho, Y. Woo and C. Bae. "Improvement of DME HCCI engine combustion by direct injection and EGR," *Fuel*, vol. 113, pp. 617-624, 2013.
- [4] F. Foucher, P. Higelin, C. Mounaïm-Rousselle and P. Dagaut. "Influence of Ozone on the Combustion of n-Heptane in a HCCI Engine," *Proceedings of the Combustion Institute*, vol. 34, no 2, pp. 3005-3012, 2013.
- [5] H. S. Yücesu, T. Topgöl, C. Cinar, and M. Okur. "Effect of ethanol-gasoline blends on engine performance and exhaust emissions in different compression ratios," *Applied Thermal Engineering*, vol. 26, no 17, pp. 2272-2278, 2006.

- [6] R. C. Costa, and J. R. Sodr . "Compression ratio effects on an ethanol/gasoline fuelled engine performance," *Applied Thermal Engineering*, vol. 31, no 2, pp. 278-283, 2011.
- [7] P. M. Najt and D. E. Foster. "Compression-ignited homogeneous charge combustion," *SAE Technical paper*, 1983.
- [8] N. Iida and T. Igarashi, "Auto-ignition and combustion of n-butane and DME/air mixtures in a homogeneous charge compression ignition engine," *SAE Technical Paper*, 2000.
- [9] C. Sayin and M. Gumus. "Impact of compression ratio and injection parameters on the performance and emissions of a DI diesel engine fueled with biodiesel-blended diesel fuel," *Applied thermal engineering*, vol. 31, no 16, pp. 3182-3188, 2011.
- [10] S. S. Karhale, R. G. Nadre, D. K. Das and S. K. Dash. "Studies on comparative performance of a compression ignition engine with different blends of biodiesel and diesel under varying operating conditions," *Karnataka Journal of Agricultural Sciences*, vol. 21, no 2, 2010.
- [11] S. Puhan, R. Jegan, K. Balasubramanian and G. Nagarajan. "Effect of injection pressure on performance, emission and combustion characteristics of high linolenic linseed oil methyl ester in a DI diesel engine," *Renewable Energy*, vol. 34, no 5, pp. 1227-1233, 2009.
- [12] J. B. Heywood. "Internal combustion engine fundamentals," *New York: McGraw-Hill*, 1988.
- [13] G. Woschni. "A universally applicable equation for the instantaneous heat transfer coefficient in the internal combustion engine," *SAE Technical paper*, 1967.
- [14] M. Yanbin. "HCCI Heat Release Rate and Combustion Efficiency: A Couple KIVA Multi-Zone Modeling Study," *ProQuest*, 2008.
- [15] E. A. Ajav, B. Singh and T. K. Bhattacharya. "Performance of a stationary diesel engine using vapourized ethanol as supplementary fuel," *Biomass and Bioenergy*, vol. 15, no 6, pp. 493-502, 1998.
- [16] T. D'Andrea, P. F. Henshaw and D. K. Ting. "The addition of hydrogen to a gasoline-fuelled SI engine," *International Journal of Hydrogen Energy*, vol. 29, no 14, pp. 1541-1552, 2004.
- [17] B. Challen and R. Baranescu, "Diesel engine reference book," *McFarland*, 1999.